AN AERIAL RADIOLOGICAL SURVEY OF THE LOS ALAMOS NATIONAL LABORATORY AND SURROUNDING AREA

LOS ALAMOS, NEW MEXICO
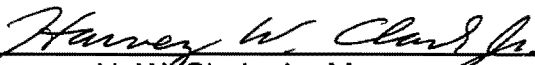
DATE OF SURVEY: APRIL – MAY 1994

DISCLAIMER

AN AERIAL RADIOLOGICAL SURVEY OF THE LOS ALAMOS NATIONAL LABORATORY AND SURROUNDING AREA

LOS ALAMOS, NEW MEXICO

DATE OF SURVEY: APRIL – MAY 1994

L. V. Singman
Project Scientist

REVIEWED BY

H. W. Clark, Jr., Manager
Radiation Sciences Section

This Document is UNCLASSIFIED

D. Wright
Authorized Derivative Classifier

ABSTRACT

A team from the Remote Sensing Laboratory conducted an aerial radiological survey of the Los Alamos National Laboratory, Los Alamos, New Mexico, during April 20 to May 4, 1994. The survey team measured the terrestrial gamma radiation at the site to determine the levels of natural and man-made radiation. This survey included the areas covered by a previous survey conducted in 1982.

The results of the aerial survey showed a background exposure rate that varied from 7 to 17 microroentgens per hour (μR/h) plus an approximate 7.5-μR/h contribution from cosmic rays. The major radioactive isotopes found in this survey were potassium-40, thallium-208, bismuth-212, bismuth-214, and actinium-228, which are all naturally occurring isotopes, and sodium-24, manganese-54, cobalt-58, cobalt-60, cesium-134, cesium-137, excess thallium-208, protactinium-234m, and americium-241, which are due to human actions in the survey area. In regions away from man-made activity, the exposure rates inferred from gamma-ray measurements from this survey agree closely with the exposure rates inferred from the 1982 survey.

CONTENTS

Figures

Tables

Appendices

1.0 INTRODUCTION

The Atomic Energy Commission, a predecessor of the U.S. Department of Energy (DOE), began a program in 1958 to map the terrestrial gamma radiation in and around facilities that produce, use, or store radioactive materials. The Aerial Measuring System (AMS) evolved from this program.

The AMS is an aerial surveillance system used in detecting nuclear radiation. The AMS is used to ensure public safety from man-made nuclear radiation by monitoring potential sources of radiation such as nuclear power plants, plants where nuclear materials are manufactured, and sites of former nuclear detonations. The AMS is maintained by the DOE and has been operated by Bechtel Nevada since January 1,1996, under contract to the DOE. During this survey, the AMS was operated by EG&G Energy Measurements, Inc. (EG&G/EM). The AMS is operated from two sites, the Remote Sensing Laboratory (RSL) located at Nellis Air Force Base in Las Vegas, Nevada, and the Washington Aerial Measurements Operations located at Andrews Air Force Base near Washington, D.C. Bechtel Nevada routinely conducts aerial surveys for the DOE, U.S. Nuclear Regulatory Commission, and other government agencies.

During April 20 to May 4, 1994, a team from the RSL conducted an aerial radiological survey of the Los Alamos National Laboratory (LANL). The DOE requested this follow-up survey to assess the impact of the past 12 years of operation.

Although the laboratory has been the subject of numerous radiological studies by both LANL[1-4] and EG&G/EM,[5-8] a comprehensive, detailed radiation map of the entire area has never been published. The object of this survey was to systematically map both the natural and man-made gamma radiation of the entire laboratory area.

The most recent aerial radiation survey prior to 1994 was conducted with a helicopter in September 1982. That survey resulted in two reports,[5,6] together covering about 20 percent of the laboratory area. One report covered Technical Area 15 (TA-15); the other report covered TA-2, TA-21, and TA-53. An RSL aerial survey was also conducted in 1975 with a helicopter,[7] but a report was not published.

An earlier radiological survey[8] conducted in 1961–1962 was also performed at the LANL area. An airplane (rather than a helicopter) was flown at 152 m (500 ft) above the ground, with nominal 1.6-km (1-mi) line spacing to cover an area approximately 160 km (100 mi) wide by 250 km (160 mi) long. The equipment on board the airplane recorded only the number of gamma-ray counts each second and did not measure the energy of the gamma rays. The exposure rates inferred from the count rates of that measurement are two to three times higher than those of the present measurement. The 1961–1962 survey will not be included in later discussions due to the sparse sampling of the area during that survey (only nine flight lines intersected the survey area that was covered with 152 lines in the current survey) and the uncertainty in the conversion from count rate to exposure rate.

2.0 SURVEY SITE DESCRIPTION

The first atomic bomb was built at LANL during World War II. The laboratory now supports a wide variety of research activities in addition to the original nuclear weapons research. The activities are conducted in technical areas that are scattered throughout a 111-sq-km (43-sq-mi) federal reservation.

LANL is located in Los Alamos County in north central New Mexico about 40 km (25 mi) northwest of Santa Fe. The Los Alamos National Laboratory Reservation is situated on the Pajarito Plateau between the Jemez Mountains in the northwest and the Rio Grande Valley in the southeast. The plateau consists of a series of finger-like mesas separated by deep east–west-oriented canyons in the northern part and northwest–southeast-oriented canyons in the southern part. The canyons are 46–91 m (150–300 ft) deep and 91–183 m (300–600 ft) wide. The mesas range in elevation from about 2,400 m (7,800 ft) to about 1,900 m (6,200 ft). The vegetation consists mainly of coniferous forests and pinon-juniper bush lands that support a typical variety of western mountain wildlife. Laboratory land is used for building sites, test areas, and waste disposal and provides isolation for security and safety.

The very rugged terrain of the LANL area is shown in Figure 1. Also shown are the boundary of the aerial survey, which approximates the laboratory boundary, and the locations of man-made isotopes as indicated by the aerial gamma survey. Note that the RSL photograph has not been orthogonalized, so survey positions on the map may contain errors up to 91 m (300 ft).

The survey covered about 85 percent of the Los Alamos National Laboratory Reservation. Part of Pueblo Canyon, including the town of Los Alamos in the north

LOCATION DIAGRAM

UT   CO

AZ

SURVEY LOCATION

NEW MEXICO

MEXICO   TX
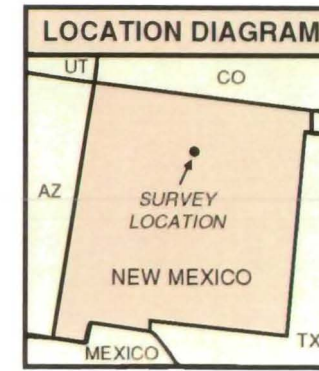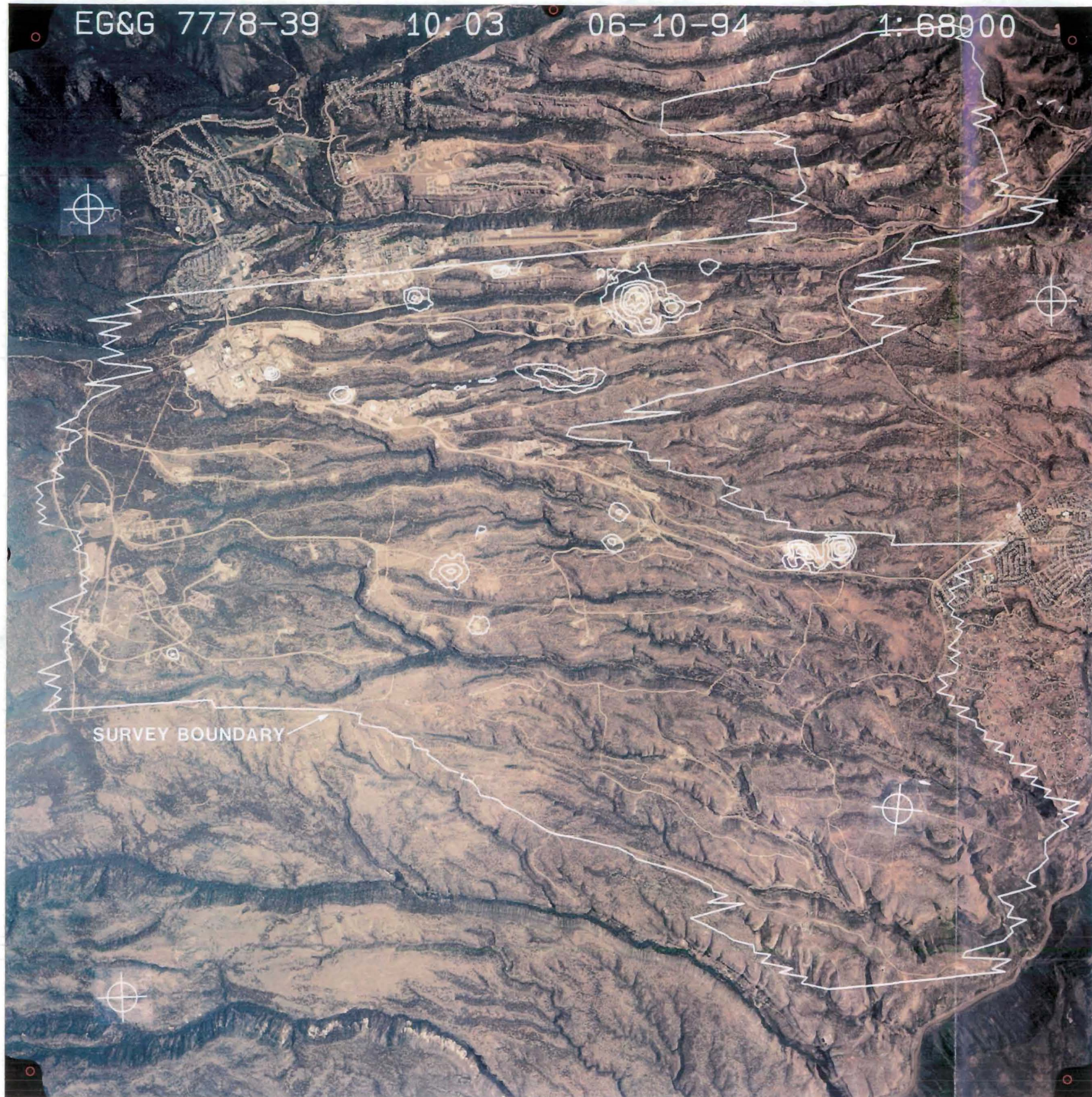
NOTE: White contoured areas indicate man-made gamma activity.

SURVEY BOUNDARY

Date of Survey: April -- May 1994
Date of Base Photo: June 10, 1994

KILOMETERS

0   1   2   3   4   5

0   1   2   3   4

MILES
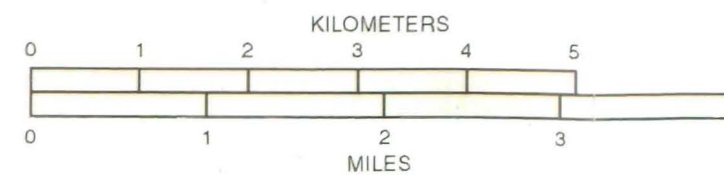
FIGURE 1.   *AERIAL PHOTOGRAPH OF THE LOS ALAMOS NATIONAL LABORATORY AND SURROUNDING AREA*

of the reservation, and a small area in the southern tip of the canyon were not covered to avoid disturbing nesting peregrine falcons, which are protected by the Endangered Species Act.

3.0 NATURAL BACKGROUND RADIATION

Throughout this report, radiation levels (exposure rates) are given in units of microroentgens per hour (μR/h). These values are defined in terms of the radiation effect on a specific quantity of air. Dose represents the amount of energy deposited in any material by the radiation. A common quantity used in radiation studies is the dose equivalent, which takes into account the biological effect of the abosrbed dose on the human body. The dose equivalent is expressed in units of rem, and for gamma rays, one μR/h of exposure rate is approximately equal to 8.37 mrem/yr.

Natural background radiation originates from several different sources. Natural terrestrial isotopes, airborne radon gas and its daughters, and cosmic rays are the three sources generally considered to comprise the natural background radiation field. Two other contributors to the full gamma-ray spectrum are man-made terrestrial isotopes and the equipment.

Long-lived radionuclides present in the earth's crust are usually the largest source of background radiation. Naturally occurring isotopes found in the soil and bedrock consist mainly of radionuclides from the uranium and thorium decay chains and radioactive potassium. The most prominent natural isotopes usually seen in aerial spectra are potassium-40 (^{40}K), 0.12 percent of natural potassium; thallium-208 (^{208}Tl) and actinium-208 (^{208}Ac), daughters in the thorium-232 (^{232}Th) chain; and bismuth-214 (^{214}Bi), a daughter in the uranium-238 (^{238}U) chain. Although it is considered a man-made radionuclide, a measurable amount of cesium-137 (^{137}Cs) is found throughout the world as a result of the atmospheric testing of nuclear weapons. These naturally occurring isotopes typically contribute 1–15 μR/h to the background radiation field.[9]

Radon (a noble gas) is a member of both the uranium and thorium decay chains. After it is created in the soil from its parent isotope, radon can diffuse through the soil and become airborne. The highly mobile radon-222 (^{222}Rn) of the uranium chain has a half-life of 3.8 days and yields a highly variable fraction to the gamma spectrum. The contribution of radon and its daughters to the background radiation field depends on several factors including the concentration of uranium and thorium isotopes in the soil, the permeability of the soil, and the meteorological conditions at the time of measurement. Typically, airborne radiation contributes 1–10 percent of the natural background radiation level.

Cosmic rays entering the earth's atmosphere are a third source of background radiation. High-energy cosmic rays (principally protons, alpha particles, and some heavier nuclei) interact predominantly with atoms in the upper atmosphere to produce showers of secondary radiation. The contribution of cosmic rays to the background radiation field varies with altitude and geomagnetic latitude. The earth's magnetic field traps some of the cosmic rays, so a larger fraction of the cosmic rays reach the poles than reach the equator. In the continental United States, values range from 3.3 μR/h at sea level in Florida to 12 μR/h at an elevation of 3,000 m (9,800 ft) in Colorado.[10]

4.0 DATA ACQUISITION

Gamma-ray data were acquired at LANL from an instrumented helicopter (Figure 2) flying parallel lines separated by 91 m (300 ft) at an altitude of 61 m (200 ft) above the ground. Some of the survey parameters are listed in Appendix A. Preflight calibration data and post flight-line data were evaluated immediately on a ground-based computer to verify integrity and to assess the LANL terrestrial gamma environment. Some 18 flights were required to complete the survey. More data-acquisition detail is given in Appendix B.

4.1 Aerial Measuring System

The aircraft system consists of the following:

A. The Messerschmitt-Bolkow-Blohm (MBB) BO-105 helicopter capable of flying from 3–3.5 hours with the instrumentation and a crew of two.

B. The sodium iodide, thallium-activated, NaI(Tl), detector pods each containing four 2- $\times$ 4- $\times$ 16-in detectors plus a 2- $\times$ 4- $\times$ 4-in detector mounted just above the closely packed larger detectors.

C. The Radiation and Environmental Data Acquisition Recorder, Version IV, (REDAR IV) system that receives, processes, displays, and records the incoming gamma, atmospheric, and positional signals.

FIGURE 2. *MBB BO-105 HELICOPTER WITH DETECTOR PODS*

D. The Real-Time Differential Global Positioning System (RTDGPS) receiver.

4.2 Mobile Data Processor

A ground-based, mobile computer system was used to process the stored gamma data both before and after each acquisition flight. Pre- and postflight processing validated the integrity of the aerial system data. This system aided the continuous creation and updating of contour maps showing the intensity of gamma radiation as the survey progressed.

4.3 Survey Procedure

A. One hundred fifty-two flight lines were planned and plotted to fit a U.S. Geological Survey topographical map of Los Alamos, New Mexico.

B. Roads and landmarks were flown in the survey area. The resulting path plot was used to scale gamma data to the map.

C. The standard individual acquisition flight profile included the following steps:

1. A preflight check of the aerial system was performed and evaluated before each flight.

2. The test line was flown at the survey altitude of 61 m (200 ft). During one flight it was flown at 61, 122, 244, 305, and 914 m (200, 400, 800, 1,000, and 2,000 ft) to determine the atmospheric gamma-ray attenuation coefficient.

3. Adjacent flight lines were flown, so coverage was continuous in time and space.

4. The test line was reflown at 61 m (200 ft).

5. A postflight computer routine was applied to the new data for quality and parameter analysis, and the gamma count-rate contour maps were updated.

D. After all the planned lines had been flown, a fraction of one line from each flight was reflown. These line data were compared to the initial data.

5.0 DATA ANALYSIS

About 31,200 data points along 152 flight lines were accumulated at 61 m (200 ft) above the LANL terrain. Each data point consisted of a 1,024-channel gamma energy spectrum, atmospheric temperature and pressure, altitude, and positional coordinates from the Global Positioning System (GPS) satellites.

The gamma energy spectra contain the radiological information that was used in the computer-aided analysis to evaluate (a) the natural gamma exposure rate at 1 meter above the ground and (b) the location, identity, and concentration of man-made isotopes. The specific variables produced are the gross count rate (GC) used to estimate terrestrial exposure rate; the man-made gross count rate (MMGC) used to locate man-made isotopes; photopeak count rates used to search for and locate specific isotopes; and net spectra used to verify the species of the detected gamma emitters.

5.1 Gross Count Rate

The total gamma interaction rate in the detectors yields the total count rate. These gammas originate in the soil and from airborne radon, cosmic interactions in the air, and the aircraft. The GC is defined as the total count rate less the radon, aircraft, and cosmic components, so it represents the soil or ground component.

$$GC = Total - (radon + cosmic + aircraft) \quad (1)$$

The measured gamma energy range has been set from 38–3,026 keV, which includes most detectable natural gammas. The lower limit is set just above electronic noise, and the upper limit includes all terrestrial gammas.

The GC has been correlated to the exposure rate, $\mu R/h$, at ground level. The correlation is

4

930 cps/(μR/h) for the LANL area flown at 61 m. This value is accurate to within about ± 1 μR/h for natural isotopes distributed in the soil and may not be applied to man-made isotopes. The GC was evaluated, contoured, and plotted for the LANL data. More details of the method are provided in Appendix C.

5.2 Man-Made Gross Count Rate

The MMGC divides the energy spectrum into two parts: part A, the integral count rate from 38–1,394 keV and part B, the integral count rate from 1,394–3,026 keV. Gammas from man-made isotopes usually appear in part A (or energy window A) whereas natural gammas appear in both A and B (energy windows A and B). This allows a simple method for separating the man-made gamma count rates from the natural gammas.

$$MMGC = A - KB \qquad (2)$$

The coefficient, K, is evaluated over the test line and over the survey area where only natural gammas exist. The MMGC was evaluated over the entire LANL survey area, then contoured, and plotted. The contour plot shows the location and magnitude of most of the man-made isotopes on the LANL site. Some man-made isotopes are not detected with this method, either because their gamma fluence rates are too low or because some of their gamma energy components lie in window B. Extensions of the MMGC method were used to locate anomalous gammas in the upper fraction of the energy spectrum (above 1,394 keV). More detail of the MMGC method is provided in Appendix C.

5.3 Photopeak Count Rates

Gamma rays from specific isotopes may be detected using a method similar to the MMGC. An energy window, A, is placed in the spectrum to evaluate those unique gamma-ray photopeaks. A background window, B, is placed where background or other species exist. An "$A - KB$" equation, evaluated over the survey area, yields increased count rates where the anticipated gamma and parent isotope exist. This method may or may not be more sensitive than the MMGC.

In some cases, two background windows were used: one at an energy higher than A and one at an energy lower than A. With the use of a second (lower-energy) window, the increase in background counts causes a slight decrease in sensitivity compared to the single background-window algorithm. The advantage of the two-background-window algorithm emerges when the shape of the gamma-ray spectrum near the photopeak is changing. Then, using a background window on each side of the photopeak produces a better estimate of the background counts present in the photopeak window.

When the terrain elevation changes rapidly from mesa to canyon, the helicopter cannot maintain both its forward speed and altitude above the ground. The resulting change in distance that the gamma ray must travel produces a spectral shape change that the two-background-window algorithm handles more accurately. Both the americium-241 (^{241}Am) and ^{137}Cs search algorithms utilized two background windows.

Other specific photopeaks, where the data were evaluated, include those for excess ^{208}Tl, protactinium-234m (^{234m}Pa), ^{214}Bi, and cobalt-60 (^{60}Co). Only ^{241}Am was not detectable from examination of the GC or MMGC plots.

Contour plots of photopeak count rates for all of the preceding isotopes were plotted to assess their existence and location in the LANL area. The accent was on the possible anomalies located outside the technical areas.

5.4 Net Gamma Energy Spectrum

Most positive count-rate excursions above three standard deviations of the MMGC or the photopeak count rates were further evaluated from net spectrum plots. The net spectrum is simply the spectrum associated with the excursion less a neighboring background spectrum.

The photopeaks in the net spectrum were then examined for those associated with man-made isotopes. A spectrum from each man-made anomaly is included in this report. Many net spectra associated with an algorithm excursion do not indicate the presence of man-made isotopes. These spectra were not included in this report unless they occurred in a technical area.

5

5.5 Data Averaging and Counting Statistics

Total count rates and photopeak count rates are evaluated and retained in raw form as data sets. However, the algorithm count rates (GC and MMGC) and photopeak count rates is generally averaged over five seconds (about 180 m [600 ft] along a flight line). That is, each set of five data points are averaged to yield a new data point at the location of the central raw point. The process is advanced one raw data point at a time, so the total number of data points remains the same.

The averaging process has the advantage of allowing a clearer picture, whether line plot or contour, to the analyst or reviewer. The five-second average produces little distortion to a point-source count-rate plot from a 61-m (200-ft) altitude, 36-m/s data set.

Background counting statistics from both MMGC and photopeak algorithms were evaluated flight by flight and over large fractions of the LANL survey area. Generally, three times the algorithm's standard deviation (3σ) of the averaged algorithm output was chosen as the value for the lowest-level contour line.

6.0 RESULTS

The primary results of this survey are the man-made count-rate map (Figure 3) and the terrestrial exposure-rate map (Figure 4). In addition, gamma energy spectra from 20 locations are presented to indicate the anomalous isotopes and the natural isotopes that are present. In areas where the radiation contours indicate a point-like source of radiation, an estimate of the source strength is presented in Table 1. Note that the gamma contours have been overlaid on a road map created by the DeLorme Mapping company's MapExpert® and contain some of the local place names.

Some isotopic source values have been estimated but suffer from inadequate knowledge of the source configuration and complexity. Detection efficiencies for the gammas and their isotopes that were detected during the survey are listed in Table 2.

Finally, not all gamma emitters were detected during the survey because the aerial system is limited to a minimum detectable activity (MDA) for each emitter. Sources having an activity smaller than this amount are unlikely to produce a count rate that is distinguishable from statistical fluctuations in the background.

The MDA as used here is three standard deviations above zero or above the background value of the algorithm output. Minimum contour levels are generally set at the MDA. Some minimum contour levels are listed in Table 3.

6.1 Man-Made Count-Rate Map

The man-made count-rate map (Figure 3) includes a MMGC map as well as portions of an excess ^{208}Tl count-rate map and an ^{241}Am count-rate map. This combined presentation depicts all of the detected anomalous gamma activity on one map. The wide-energy window MMGC algorithm was not as sensitive for detecting excess ^{208}Tl and ^{241}Am as were individual narrow-window algorithms. Those anomalies not detected by the MMGC were simply transferred from separate excess ^{208}Tl and ^{241}Am maps onto the MMGC map.

The 20 locations where anomalous gamma activity was detected are discussed individually in the following sections. Location numbers beside each anomalous area, shown in Figure 3, also identify the spectra in Figures 5–8.

6.1.1 Technical Area 2, Location 1

TA-2, Omega Site, contains two research reactors, so some man-made activity should be expected. Spectrum 1 shows the presence of both ^{137}Cs and ^{60}Co. The highest contour at 12,000 cps locates the maximum activity and one of the reactors. The lowest contour at 1,200 cps is not concentric with the other contours and suggests the active material is spatially extended. The source's photopeak count rates approximate 1 and 18 mCi of ^{137}Cs and ^{60}Co point sources, respectively.

The exposure-rate map (Figure 4)) indicates the location of this site with an exposure contour at 25–50 µR/h (an understatement). The exposure may be mostly due to ^{60}Co since its hypothetical point source value is 18 times that of the ^{137}Cs.

6.1.2 Technical Area 21, Location 2

TA-21, DP Site, between Los Alamos Canyon and DP Canyon, is the site of the plutonium and chemistry laboratories. Unfortunately, the northern boundary of the survey ends over DP Canyon, so the contour lines are not closed. Spectra 2a and 2b indicate both ^{241}Am

CONVERSION SCALE[a]

Color	MMGC Rate[b] (cps)	241Am Photopeak Count Rate[c] (cps)	208Tl Photopeak Count Rate[d] (cps)
(light blue)	1,200 – 3,800	80 – 240	100 – 160
(green)	3,800 – 12,000	240 – 480	160 – 220
(yellow)	12,000 – 38,000		220 – 280
(orange)	38,000 – 120,000		
(pink)	120,000 – 380,000		

[a] The identification of the locations numbered 1 to 20 are referenced in Table 1.

[b] Those contours, not otherwise labeled, are created from the MMGC-detection algorithm.

[c] The label Am identfies the contours due to the 241Am gammas measured in the 60-keV photopeak.

[d] The label Tl identifies the contours due to the excess 208Tl gammas measured in the 2,614-keV photopeak.

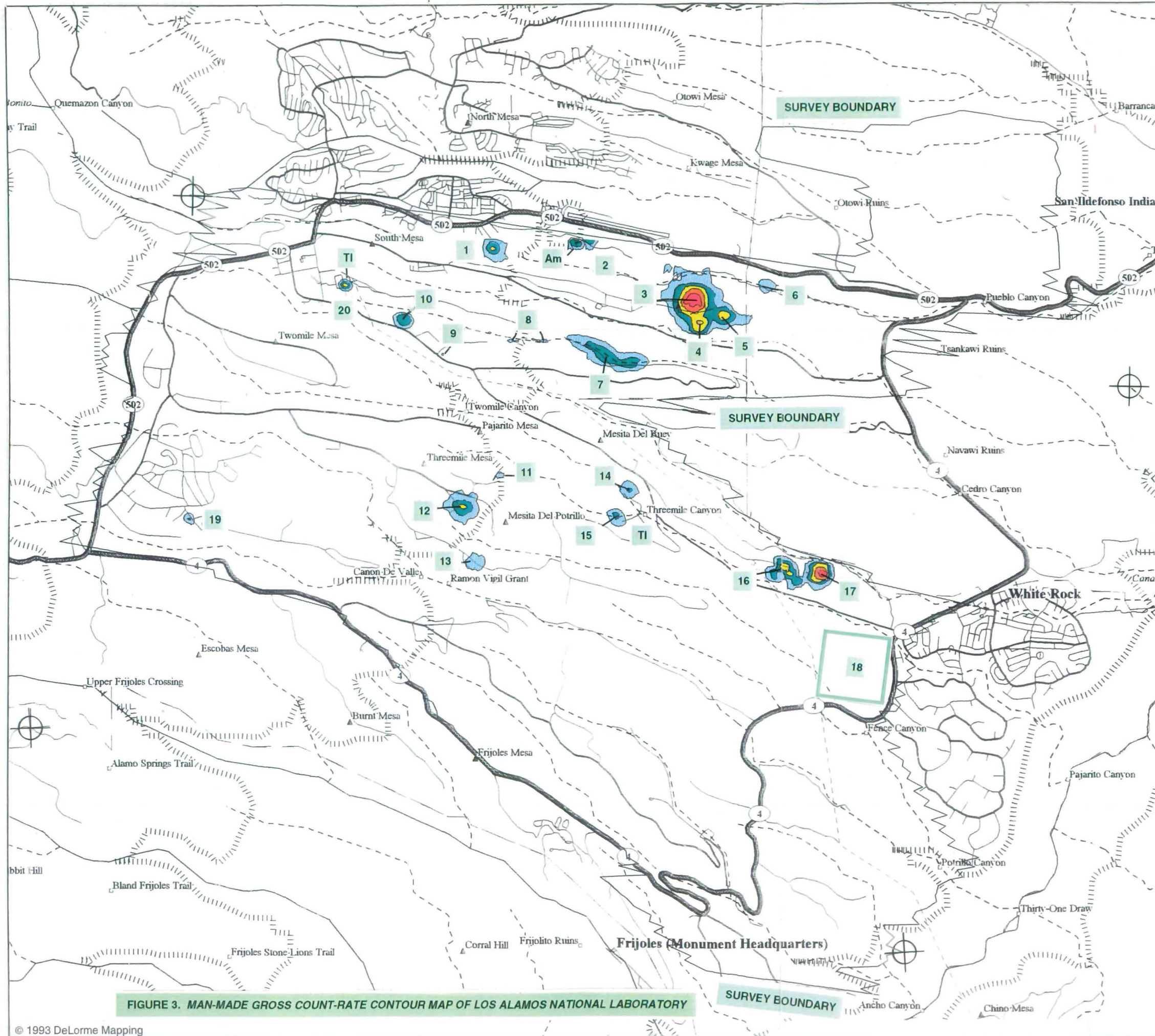**Date of Survey: April--May 1994**

LOCATION DIAGRAM

FIGURE 3. MAN-MADE GROSS COUNT-RATE CONTOUR MAP OF LOS ALAMOS NATIONAL LABORATORY

7

Road and Place Map From DeLorme XMap® Professional
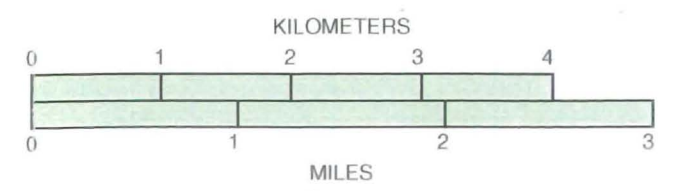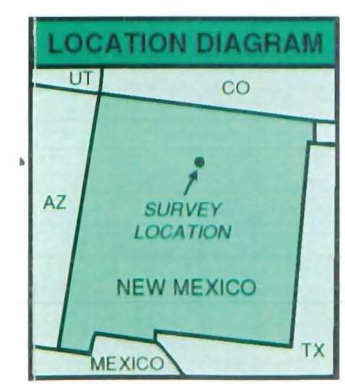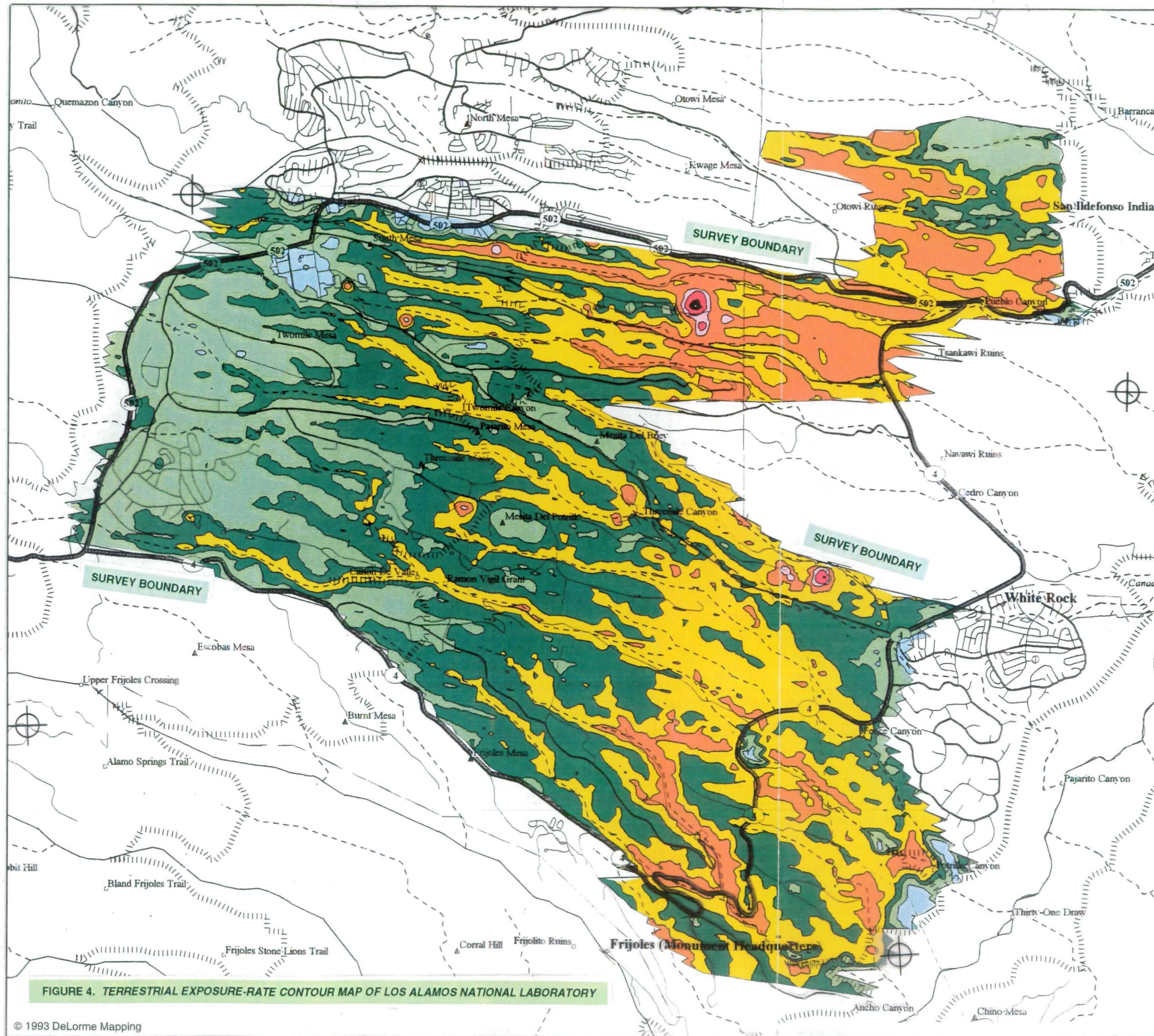
CONVERSION SCALE

Color	Terrestrial Gamma Count Rate (cps)	Terrestrial Exposure Rate at One Meter AGL[a] (µR/h)
	5,580 – 7,440	6 – 8
	7,440 – 9,300	8 – 10
	9,300 – 11,160	10 – 12
	11,160 – 13,950	12 – 15
	13,950 – 23,250	15 – 25
	23,250 – 46,500	25 – 50
	46,500 – 232,500	50 – 100
	232,500 – 465,000	100 – 500

[a] The exposure rate is inferred from gamma count-rate data measured at 61 m (200 ft) above the ground. Only the gamma fraction originating in or on the ground is presented here. The cosmic fraction, about 7.5 µR/h, and the airborne radon fraction, from 0 to 0.5 µR/h, are not included.

Date of Survey: April--May 1994

LOCATION DIAGRAM

SURVEY LOCATION

NEW MEXICO

N

KILOMETERS

MILES
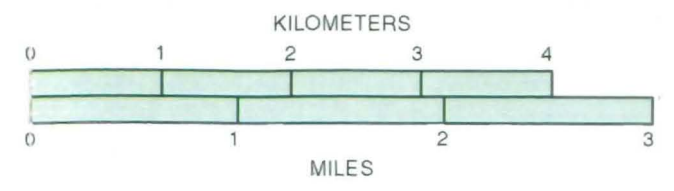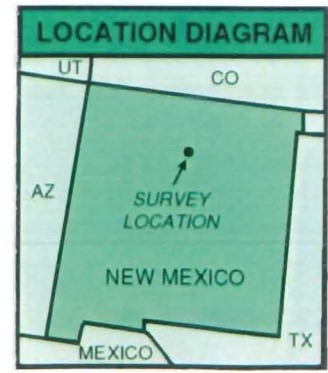
FIGURE 4. TERRESTRIAL EXPOSURE-RATE CONTOUR MAP OF LOS ALAMOS NATIONAL LABORATORY

Table 1. Summary of Man-Made Detected Sources

Location	Site Description	Identified Isotope	Point Source Strength[a] (mCi)
1	TA-2	^{60}Co	18
		^{137}Cs	1
2	TA-21	^{137}Cs	15
		^{241}Am	3
3	TA-53 LAMPF Target	^{54}Mn	2,800
		^{60}Co	800
4	TA-53 LAMPF Storage	^{54}Mn	76
		^{60}Co	32
5	TA-53 Ponds	^{22}Na	21
		^{58}Co	16
6	Los Alamos Canyon	^{137}Cs	3
7	Mortandad Canyon	^{137}Cs	b
8	Mortandad Canyon	^{137}Cs	c
9	TA-50	^{137}Cs	2
10	TA-48	511 keV	48
		^{137}Cs	d
11	TA-15 North	none	
12	TA-15 Central	^{234m}Pa	2,000
13	TA-15 South	none	
14	TA-18	^{60}Co	6
15	TA-36 Kappa Site	^{134}Cs	d
		excess ^{208}Tl	6
		^{228}Ac	d
16	TA-54 West	^{241}Am	500
17	TA-54 East	^{137}Cs	17
		^{241}Am	5,000
18	Background	^{40}K	e
		^{208}Tl	e
		^{214}Bi	e
		^{228}Ac	e
19	TA-16	^{234m}Pa	1,000
20	TA-3	^{208}Tl	8
		^{228}Ac	d

[a] A hypothetical point source is assumed. Values are rounded to the nearest millicurie.
[b] Large-area source of finite extent, Section 6.1.5.
[c] Small-area sources of unknown extent, Section 6.1.5.
[d] Highly uncertain source strength.
[e] Large-area, large-volume source.

Table 2. Detector Sensitivity to Gamma Activity in the Ground

Isotope	Gamma Energy (keV)	Area Source[a]		Point Source[b] (mCi/cps)
		For α = 0.1 cm^{-1} (pCi/g)/cps	For α = 0.001 cm^{-1} (pCi/g)/cps	
^{241}Am	59.5	0.183	0.15	0.036
Annihilation	511	0.15	0.011	0.011
^{137}Cs	662	0.026	0.017	0.023
^{134}Cs	796	0.0152	0.0094	0.016
^{58}Co	811	0.0186	0.011	0.014
^{54}Mn	835	0.015	0.0090	0.014
^{234m}Pa	1,001	2.59	1.54	2.8
	767	7.44	4.62	6.7
^{22}Na	1,275	0.0165	0.0094	0.020
^{60}Co	1,333; 1,173[c]	0.0083	0.0047	0.010
excess ^{208}Tl	2,614	0.022	0.011	0.036

[a] Vertical soil activity: $A = A_0 e^{-\alpha z}$, z = depth.
[b] On soil surface.
[c] Average energy, 1,275 keV, used in computations.

Table 3. Some Minimum Contour Activity Levels[a]

Isotope	Gamma Energy Minimum Contour		Minimum Activity[b]	
	(keV)	(3σ cps)	Area Source[c] (pCi/g)	Point Source (mCi)
^{241}Am	59.5	60	9.0	2.0
^{137}Cs	662	50	0.9	1.2
^{234m}Pa	1,001	130	200	400.
^{60}Co[d]	1,275	50	0.2	0.5
excess ^{208}Tl	2,614	100	2.0	4.0

[a] Minimum contour placed at 3σ of the search algorithm counting statistics.
[b] Values have been rounded to a single significant digit.
[c] The area source is uniformly mixed in the soil.
[d] The ^{22}Na minimum is twice that of ^{60}Co.
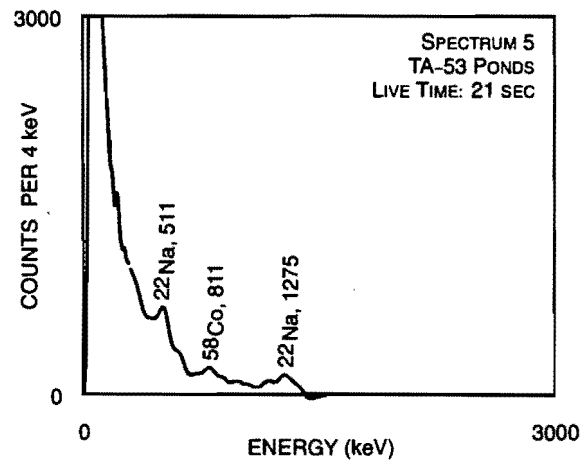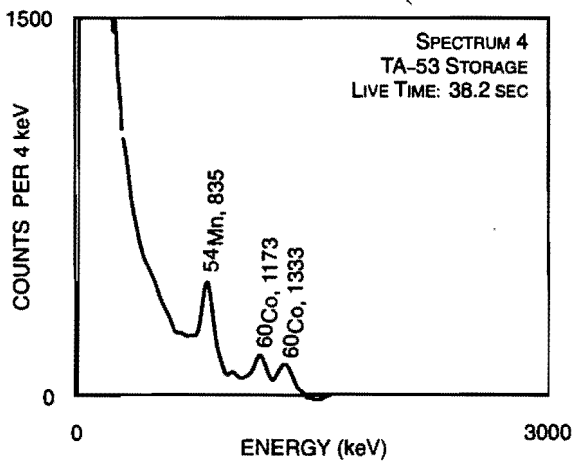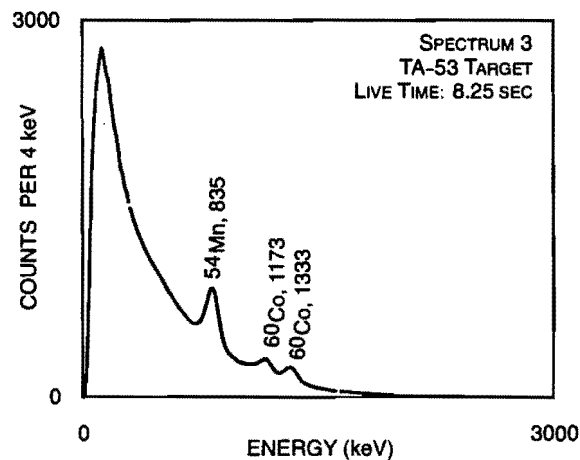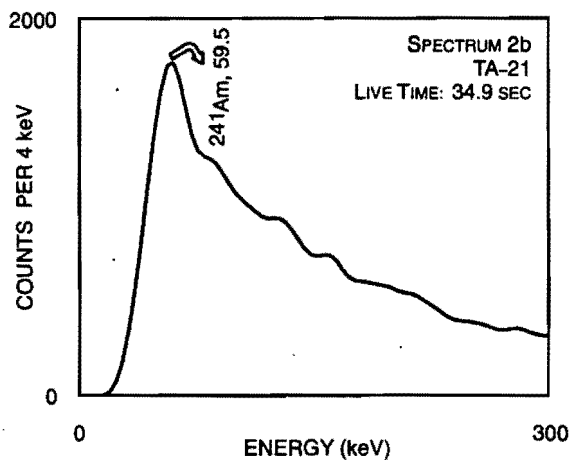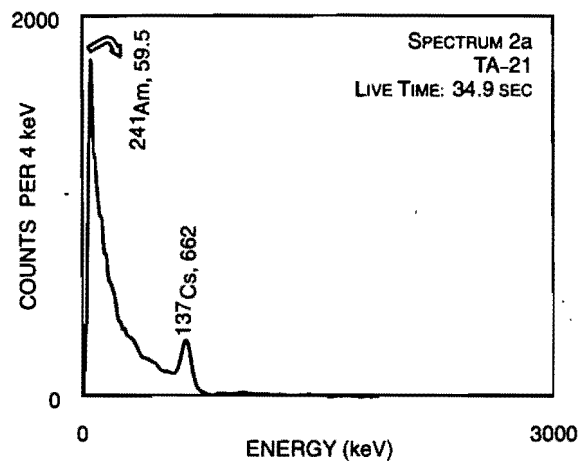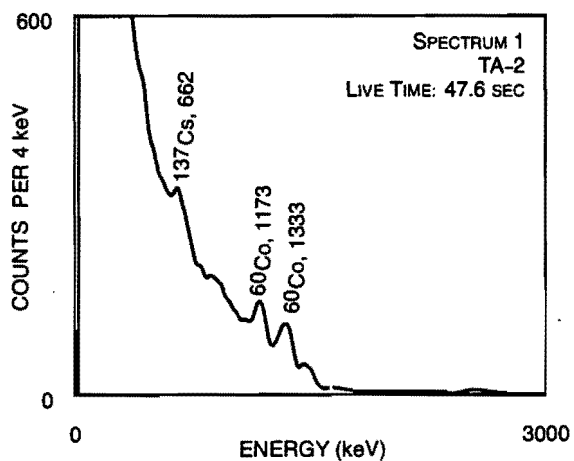
FIGURE 5. *NET GAMMA ENERGY SPECTRA FROM ANOMALOUS ACTIVITY AT THE LOS ALAMOS NATIONAL LABORATORY, LOCATIONS 1 THROUGH 5*
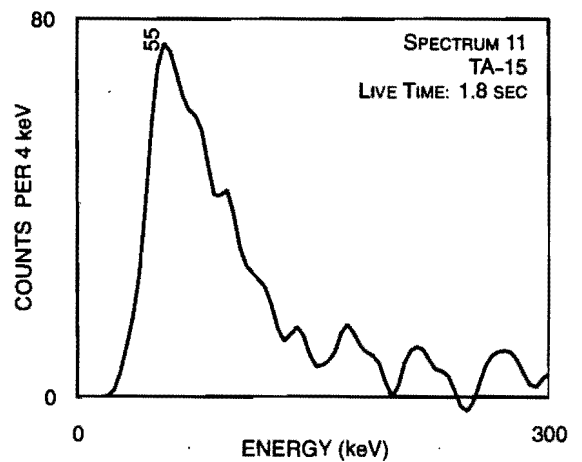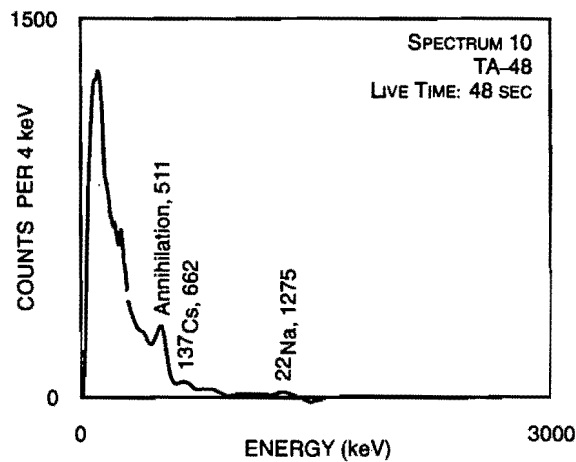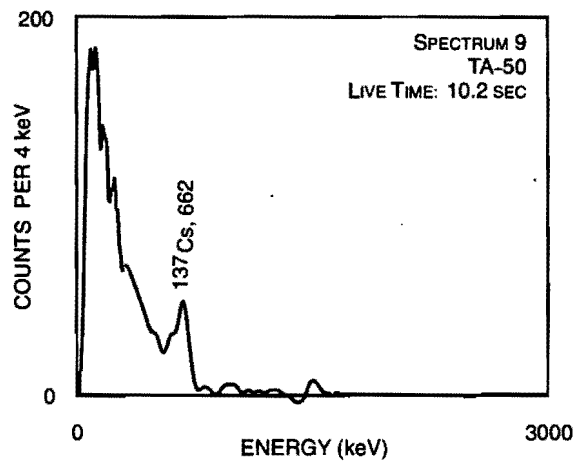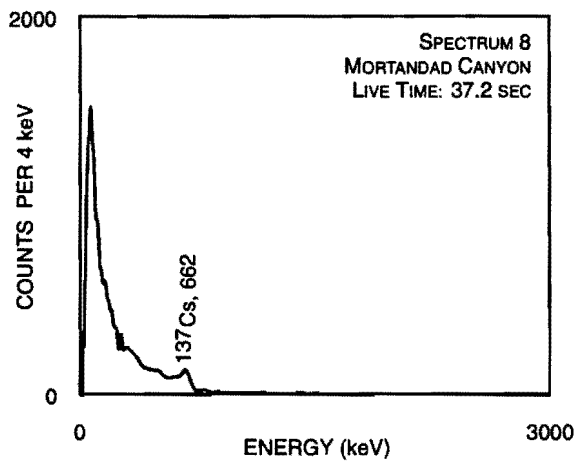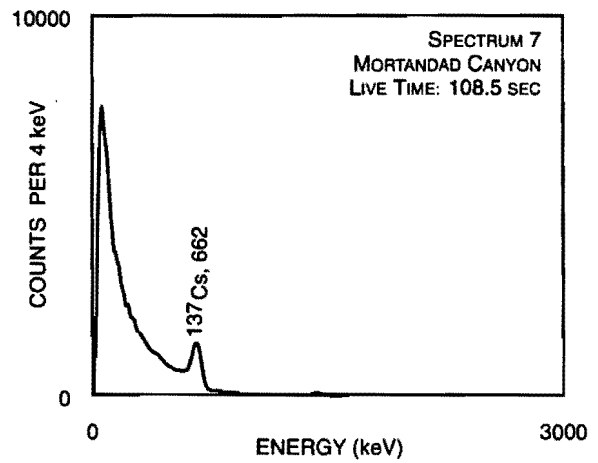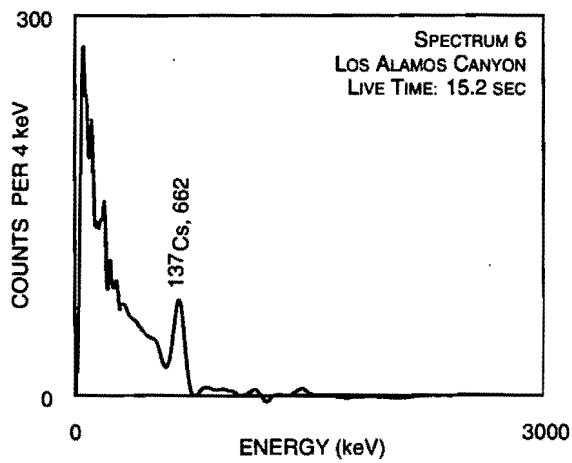
FIGURE 6. *NET GAMMA ENERGY SPECTRA FROM ANOMALOUS ACTIVITY AT THE LOS ALAMOS NATIONAL LABORATORY, LOCATIONS 6 THROUGH 11*

12
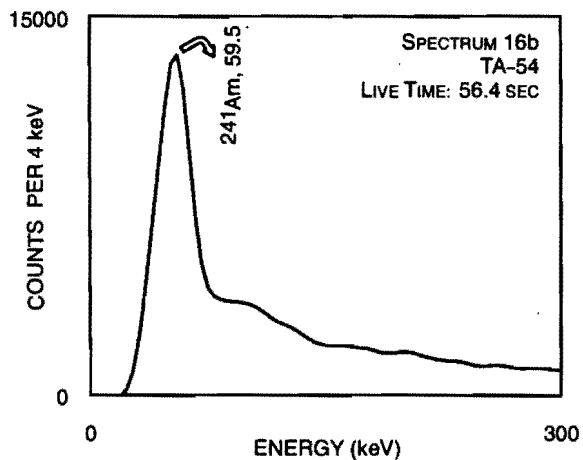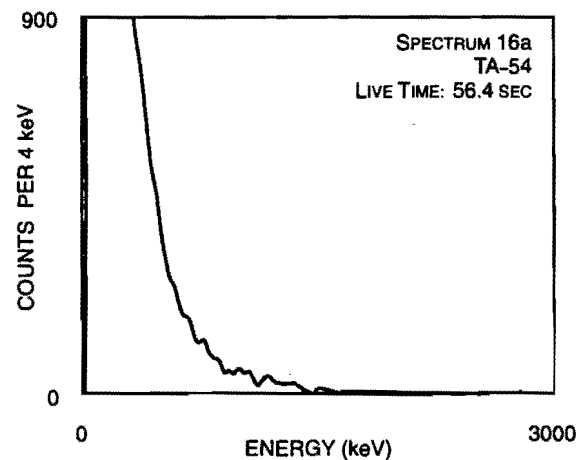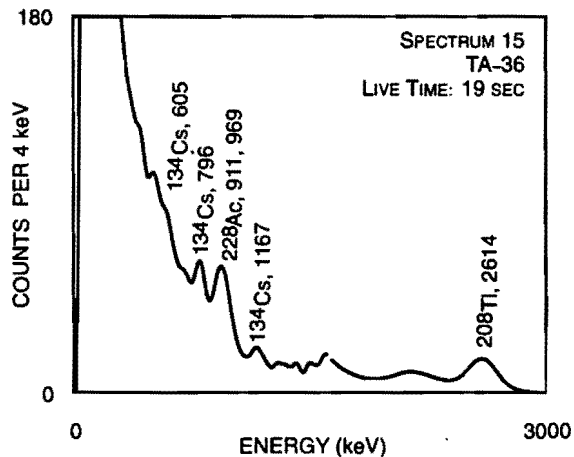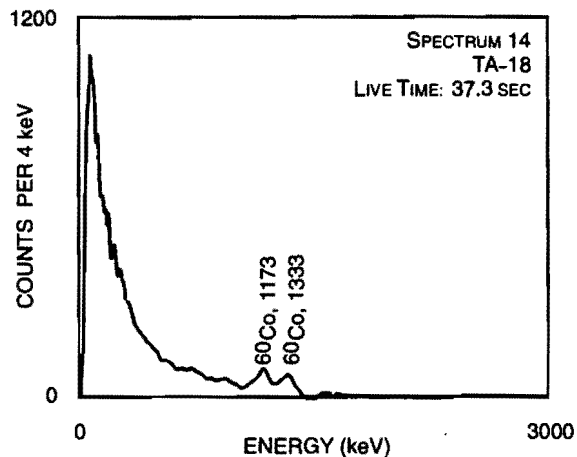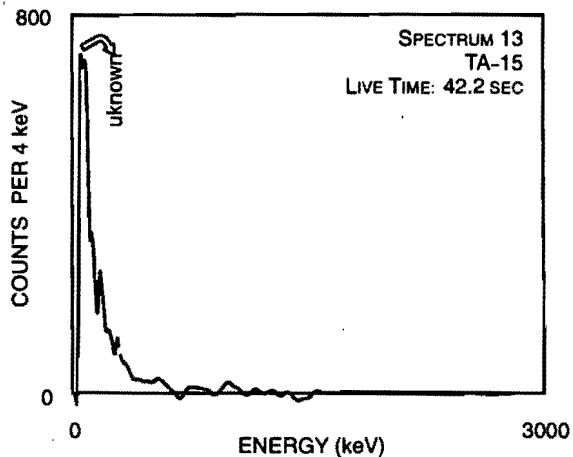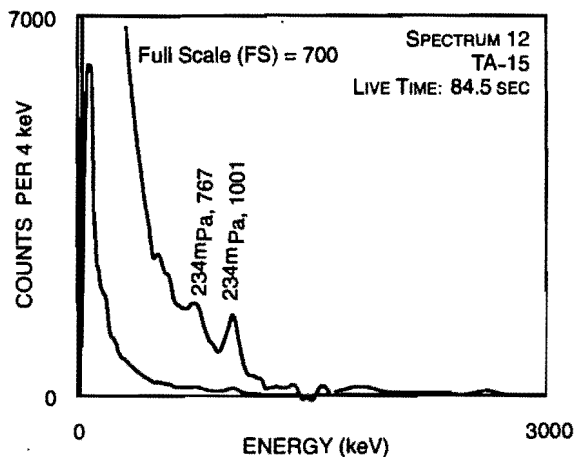
FIGURE 7. *NET GAMMA ENERGY SPECTRA FROM ANOMALOUS ACTIVITY AT THE LOS ALAMOS NATIONAL LABORATORY, LOCATIONS 12 THROUGH 16*
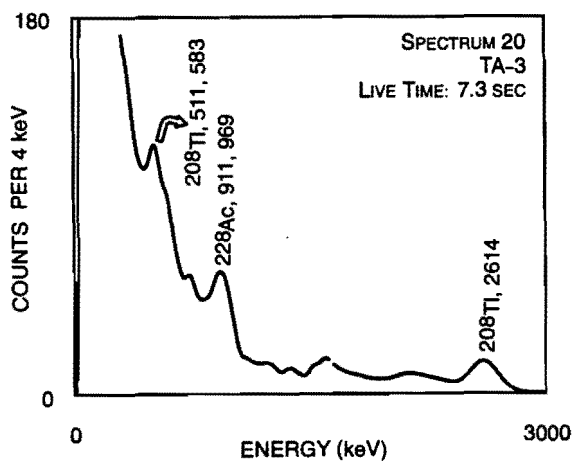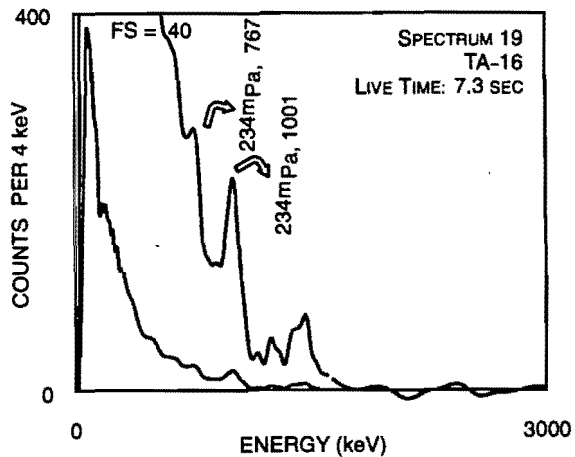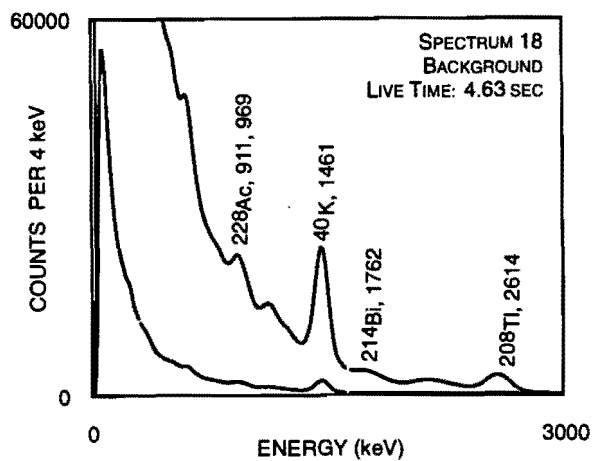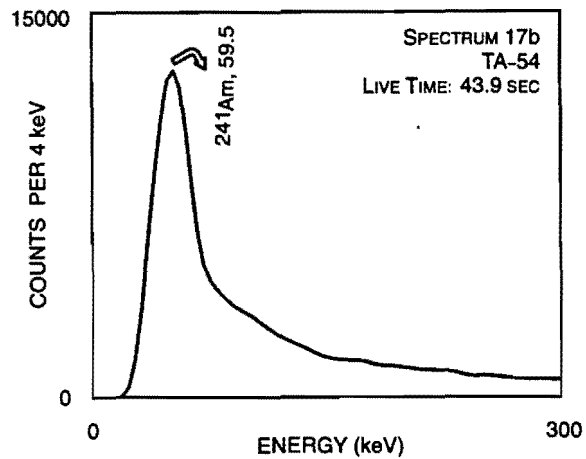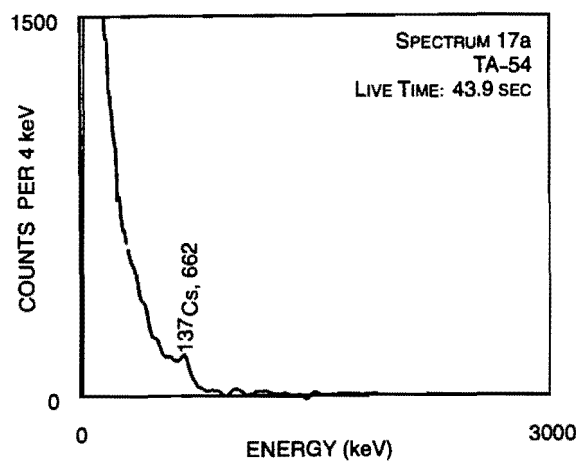
FIGURE 8. *NET GAMMA ENERGY SPECTRA FROM ANOMALOUS ACTIVITY AT THE LOS ALAMOS NATIONAL LABORATORY, LOCATIONS 17 THROUGH 20*

14

and ^{137}Cs at this site. The man-made count-rate contours (Figure 3) indicate ^{241}Am in the western part of TA-21 and ^{137}Cs in the DP Canyon between the western and eastern parts of the site. Hypothetical point sources of 2.6 and 14.6 mCi, respectively, would produce the same photopeak count rates in the detectors.

The exposure-rate map (Figure 4) indicates only the presence of ^{137}Cs (and not ^{241}Am) at 15–25 μR/h. This is an underestimate since the exposure calibration has been measured and computed for large-area sources only.

6.1.3 Technical Area 53, Locations 3, 4, and 5

The Los Alamos Meson Physics Facility (LAMPF) in TA-53 exhibits the largest gamma source detected by the airborne system at LANL. The high-energy proton beam may well be expected to produce primary and secondary nuclear reactions and consequent radioactivity. There were no radioactive air emissions from LAMPF during the survey of that region of the laboratory.

Target Area

The target area, Location 3, produces GC rates greater than 120,000 cps in the primary detectors, which puts them in a saturated condition. The single detector has been used to evaluate GC rates greater then 30,000 cps. Both manganese-54 (^{54}Mn) and ^{60}Co (2,800- and 800-mCi hypothetical point sources) are visible in Spectrum 3. Note that the lowest contour extends into the Los Alamos Canyon, and either may indicate activity deposited there or may simply be radiation originating from the target area itself. Net energy spectra from the canyon indicate no man-made isotopes. The maximum exposure rate indicated in the target is 250 μR/h, a large understatement since exposures are computed for large-area natural sources.

Storage Area

The LAMPF storage area, Location 4, exhibits much less activity than does the target area. Spectrum 4 shows the presence of ^{54}Mn and ^{60}Co (76- and 32-mCi point sources).

The maximum exposure level that is indicated is somewhat greater than 50 μR/h, but again it is an understatement. Perhaps 100 mR/h is the order of

magnitude expected a few feet above the storage area.

Pond Area

The pond area, just east of the target and storage areas, is the weakest detectable gamma source at the LAMPF. The gamma energy spectrum, Location 5, shows sodium-22 (^{22}Na) at 21 mCi and, rather weakly, cobalt-58 (^{58}Co) at 16 Ci. Note that the lowest-man-made contour, 1,200 cps, shows activity extending about 150 m (2,000 ft) in an easterly direction from the ponds.

The exposure-rate map indicates a maximum exposure somewhat larger than 25 μR/h over the ponds but is probably in the milliroentgens-per-hour range.

6.1.4 Los Alamos Canyon, Location 6

The MMGC (Figure 3) shows activity in the Los Alamos Canyon about 1 km (3,000 ft) east of the LAMPF target area and 800 m (2,000 ft) northeast of the LAMPF ponds. Spectrum 6 indicates ^{137}Cs. A point source of 3 mCi would yield the same maximum photopeak count rate. Should the ^{137}Cs isotopes be mixed in the soil, one may expect an average activity on the order of 2 picocuries per gram (pCi/g). The exposure-rate map does not indicate anything unusual in this area because the maximum exposure rate from this source is expected to be less than 1 μR/h for the uniform distribution of ^{137}Cs in the soil.

6.1.5 Mortandad Canyon, Locations 7 and 8

Mortandad Canyon contains ^{137}Cs along approximately 2 km (2 mi) of its length. The net gamma energy Spectrum 7 shows predominantly ^{137}Cs. Photopeak count rates suggest 9 pCi/g of ^{137}Cs assuming a uniform distribution in the soil. Such a concentration yields about 4 μR/h. The exposure-rate map shows a 15–25-μR/h region that tends to follow the man-made contours in Location 7. Location 8 just reaches the 15-μR/h level.

Location 8 includes 1,500 m (5,000 ft) of Mortandad Canyon to the west of Location 7 and shows only intermittent ^{137}Cs activity on the MMGC map. Spectrum 8 confirms the presence of ^{137}Cs.

6.1.6 Technical Area 50, Location 9

A small ^{137}Cs source (equivalent to a 1.5-mCi point source) exists just off Pajarito Road near TA-50,

15

Waste Management Site. Spectrum 9 confirms the ^{137}Cs identification.

6.1.7 Technical Area 48, Location 10

TA-48, Radiochemistry Site, appears as concentric circles on the man-made map, much as a point source. Spectrum 10 shows a predominant 511-keV photopeak probably due to beta annihilation. The equivalent point-source strength is 48 mCi. Cesium-137 is apparent at perhaps 1 mCi. Sodium-22 and ^{58}Co may also be present but are difficult to identify in the spectrum. At least some of the 511-keV gammas may originate in the ^{22}Na. The exposure map indicates a maximum of approximately 50 μR/h, but one should expect exposures 1,000 times greater than the map indicates since the gammas appear to originate from a small area.

6.1.8 Technical Area 15, Locations 11, 12, and 13

The man-made gamma map shows three anomalies in TA 15, R Site: (a) a central area, Location 12; (b) a southern low-activity area, Location 13; and (c) a northern very low-activity area, Location 11. The count-rate intensities decrease in the same order. These areas are separated by 700–900 m (2,000–3,000 ft).

Only the central area, the most intense, yields recognizable photopeaks in Spectrum 12. The 767- and 1,001-keV photopeaks are quite visible. Count rates from a two-window ^{234m}Pa search algorithm suggest 2 Ci of ^{234m}Pa, and thus ^{238}U may occupy Location 12.

Locations 11 and 13 are both weak sources (if they exist). Energy spectra from these locations, Spectrum 11 and Spectrum 13, yield no clear indications of the isotopes involved. However, the ^{234m}Pa photopeak search algorithm yields a contour over both Location 11 and Location 13 suggesting ^{234m}Pa exists there.

Location 12 appears on the exposure-rate map at a maximum of 25 μR/h. Again, this exposure may be an underestimate by a factor of 100–1,000.

6.1.9 Technical Area 18, Location 14

Critical assemblies in TA-18, Pajarito Laboratory Site, yield detectable activation gammas as shown by the

^{60}Co in Spectrum 14. On the exposure-rate map, this area is indicated by a closed contour of 15–25 μR/h, which may be 1,000 times lower than the actual exposure rate.

6.1.10 Technical Area 36, Location 15

TA-36, Kappa Site, shows a maximum excess ^{208}Tl contour of 170 cps (equivalent to a 6-mCi point source) using a two-window ^{208}Tl search algorithm. Spectrum 15 shows a preponderance of ^{232}Th daughter photopeaks, ^{208}Tl and ^{228}Ac. Other gamma emitters appear in this energy spectrum. Cesium-134 is a possibility although the large peak at 800 keV may be caused by other isotopes. The exposure-rate map indicates the area with a closed contour at 15–25 μR/h.

6.1.11 Technical Area 54, Locations 16 and 17

The materials waste disposal sites at TA-54 display high-level contours on both the man-made count-rate and exposure-rate maps. The predominant isotope, ^{241}Am, (in the curie range or more) is quite clear in both Spectra 16b and 17b. Spectrum 16a indicates that the large sources have saturated the detectors. Spectrum 17a shows the presence of some ^{137}Cs (equivalent to 17 mCi).

6.1.12 White Rock Area Background, Location 18

A gamma spectrum, Spectrum 18, accumulated over the area just west of the White Rock and Pajarito Acres illustrates the general components of a background spectrum for the area in and around LANL. Potassium-40 (1,461 keV) is the predominant photopeak. The ^{232}Th chain of gamma emitters is indicated by the presence of ^{208}Tl (2,614 keV) and ^{228}Ac (911 and 969 keV). Finally, ^{214}Bi indicates the presence of ^{238}U. These radioisotopes are all natural and have been detected by the aerial system throughout the United States.

6.1.13 Technical Area 16, Location 19

A concentration of ^{234m}Pa (1,000 mCi or more) is apparent in both the man-made count-rate map and the exposure-rate map for TA 16, S Site. The ^{234m}Pa is a decay product from ^{238}U, so uranium is also present. Spectrum 19 indicates the two ^{234m}Pa photopeaks always found with concentrated ^{238}U.

6.1.14 Technical Area 3, Location 20

The gamma spectrum, Spectrum 20, from the main technical core area of LANL, TA-3, contains one primary detectable gamma source, excess ^{208}Tl equivalent to an 8-mCi point source, and several other photopeaks of the ^{232}Th chain. Both the man-made count-rate map and the exposure-rate map show the presence of this anomaly.

6.2 Terrestrial Exposure-Rate Map

The terrestrial exposure-rate map (Figure 4) indicates the exposure rate at 1 meter above ground level (AGL) from the soil and surface gamma sources. This map does not include the exposure due to cosmic rays or airborne radon. These exposure values are nominally 7.5 ± 0.5 and 0.5 ± 0.5 μR/h, respectively. The radon gamma background continually changed, ranging from $0-1$ μR/h during the survey.

The general character of the exposure-rate map suggests the natural or background rate is about 10 μR/h in the west and increases to $12-25$ μR/h in the east. The canyons are also apparent from their higher-count rates (yellow and orange strips). Larger-exposure rates in the canyons are probably due to more gamma activity in the lower strata and more soil surface exposed to the detectors at a smaller average distance.

Concentric contours locate higher-exposure rates over a number of technical areas. These have been discussed in the previous sections. Note that exposure values over finite area sources (less than 300 m [1,000 ft] in diameter) are underestimated by as much as a factor of 1,000.

7.0 CONCLUSIONS

Approximately 111 sq km (43 sq mi) of the Los Alamos National Laboratory Reservation were surveyed for DOE in April and May of 1994. The 152 flight lines (a path of 1,130 km [700 mi]) spaced 91 m (300 ft) apart indicate no observable changes in the natural background gamma radiation environment. The gamma environments from laboratory technical areas occur at the same locations as were observed in the prior aerial surveys in 1982 and 1975, with the exception that some activity has virtually disappeared.

Terrestrial (natural) exposure rates agree well with the 1982 measured values in TA-15 but are somewhat higher in the Los Alamos Canyon. However, the 1982 exposure algorithm used only the upper portion of the gamma energy spectrum because of the airborne low-energy activity in the LAMPF area at that time. Note that natural exposure, as defined here, is due to that gamma fluence coming from the soil.

The ^{137}Cs activity appears to have declined since 1982. Only a single perturbation shows in the Los Alamos Canyon in the current survey. The photopeak count rate (200 cps) at that location 800 m (3,000 ft) northeast of the LAMPF ponds is somewhat less than the $240-500$ cps obtained in 1982 on a less sensitive system.

TA-15 has also changed since 1982. The most intense area of the three active areas remains easily detectable due to ^{234m}Pa gamma rays, but the north and south areas (Locations 11 and 13, Figure 3) are much weaker than in 1982. Man-made activity may not exist in these locations since no such identifiable gamma-ray photopeaks appear in their gamma energy spectra.

Eleven technical areas are detectable from the aerial system. These range in activity from an equivalent point source of a few microcuries at TA-50 to multi-curie levels at the LAMPF and TA-54. Some 2.2 percent of the surveyed area contains detectable gamma count rates from man-made activity.

APPENDIX A

SURVEY PARAMETERS

Survey Site: Los Alamos National Laboratory
Los Alamos, New Mexico

Base of Operation: Santa Fe Municipal Airport
Santa Fe, New Mexico

Survey Dates: April 20–May 4, 1994

Survey Area: 111 sq km (43 sq mi)

Site Elevation: 1,900–2,400 m (6,200–7,800 ft)

Survey Altitude: 61 m (200 ft)

Aircraft Speed: 36 m/s (70 knots)

Line Spacing: 91 m (300 ft)

Line Direction: Rotated 9 degrees clockwise from east–west

Detector Arrays: Eight (2- $\times$ 4- $\times$ 16-in) NaI(Tl) detectors
One (2- $\times$ 4- $\times$ 4-in) NaI(Tl) detectors

Acquisition System: REDAR IV

Aircraft: MBB BO-105 Helicopter (Tail Number N40EG)

Navigation System: Real-Time Differential Global Positioning System

APPENDIX B

DATA ACQUISITION

This appendix presents general data-collecting procedures that are in use. These procedures are intended to give the reader a general overview of the processes.

B.1 AERIAL MEASURING SYSTEM

The helicopter, which carries the detectors over the survey area, is flown at a nominal altitude of 61 m (200 ft) AGL. A radar altimeter system continuously monitors and provides feedback to the pilot. A line spacing of 91 m (300 ft) provides an adequate amount of overlap in the detectors' fields of view during each flight line. The lines are roughly parallel to the axes of most of the canyons traversing the survey area. Flying the helicopter parallel to the canyons minimizes the altitude adjustments that the pilot must make. Appendix A provides a summary of the survey parameters.

A navigational system, called the RDGPS, on board the helicopter determines the helicopter's position each second by receiving signals from a constellation of GPS satellites. Every four seconds, an RDGPS base station (programmed with its own true position) determines its position from the available satellites and broadcasts a positional correction to the helicopter. The correction term adjusts the helicopter's position, minimizing the errors caused by using only the satellites to determine position.

With the RDGPS positional data and the coordinates of the intended flight lines, the on-board computer reports the distance to the desired flight line every second. With the base-station correction applied, the uncertainty in the helicopter's position is ±5 m (15 ft). The second-by-second position of the helicopter is converted into the x−y coordinate system for the survey and recorded with the rest of the data on magnetic tape.

Two aluminum pods, each containing four down-looking and one up-looking NaI(Tl) detectors, are mounted to the skids of the helicopter. The eight rectangular detectors view the total radiation field available to the helicopter. One of the smaller up-looking detectors does not view the ground and is used to monitor the airborne radon and cosmic-ray contributions to the radiation field.

The down-looking detectors have a large gamma-ray sensitive volume, each detector measuring 5 × 10 × 40 cm (2 × 4 × 16 in). A small check source produces voltage pulses in each of the eight down-looking detectors. These pulses are matched in amplitude before each flight. The pulses are then added using summing amplifiers and the summed pulse is fed into an analog-to-digital converter (ADC). A second ADC is used to process the gamma signals from just one of the eight detectors to increase the linear count-rate range.

The ADCs are components of the REDAR IV system. The digital data are stored in the REDAR IV memory in 1-second intervals and written on magnetic tape at the end of each 4-second period. The REDAR IV also continuously processes and stores data from various sensors such as those for atmospheric pressure, outside air temperature, aircraft altitude, and positional data from the GPS.

B.2 SURVEY PROCEDURES

Since the detectors measure the radiation field at the altitude of the helicopter, a correction must be applied for the attenuation of the gamma-ray intensities through the air to obtain an inferred exposure rate at 1 meter AGL. One factor that strongly affects the measurement is the presence of liquid water between the radiation source and the detectors. Changes in the relative humidity of the air (water vapor) are not of concern here since the gamma-ray absorption for even 100 percent relative humidity is not that much different than for dry air. However, changes in the amount of water in the top several centimeters of the soil can introduce major discrepancies. For this reason, no data are collected immediately after a rain storm. During the LANL survey, there were five days with precipitation. The storms caused survey operations to be discontinued for the remainder of those days. However, the ground was dry enough by the next day to permit the survey to continue. More flight time was lost due to high winds than was lost due to wet grounds.

One of the first flights flown on a survey is the "perimeter" flight. This flight generally involves flying the helicopter along roads, fences, or other distinct structures that can be seen from the aircraft and are present on either U.S. Geological Survey maps or aerial

photographs. The perimeter flight establishes a link between the positional coordinates of the survey data and the aerial photographs or geographical maps used later to display the data. Since the flight is known to have followed the roads or other structures, the data coordinates can be scaled to match most distortions in the map or photograph.

While at the survey site, several flights are flown to collect data that are used for estimating the background for the radiation measurements. A "test line" is a flight path chosen near or within the survey area that has no man-made radiation sources nearby and, preferably, can be flown at the start and end of each survey flight using only visual landmarks. At the beginning of the survey, and usually again near the end of the survey, an "altitude profile" flight is flown over the test line at various altitudes to obtain a profile of the count rate as a function of altitude. For this survey, the altitudes for these measurements were 61, 122, 244, 305, and 914 m (200, 400, 600, 800, 1,000, and 3,000 ft). These data determine the air attenuation coefficient and the initial background count rate at the survey altitude. The count rate measured at each altitude is fit to an equation of the following form:

$$(C_i - B) = T \ e^{-AH_i}$$

where

C_i = the gamma-ray count rate measured at each altitude (cps)

B = the background count rate from nonterrestrial sources to be determined (cps)

T = the gamma-ray count rate from terrestrial sources (cps)

A = the air attenuation coefficient to be determined (m^{-1})

H_i = the aircraft height above the ground during the measurement (m)

A background count rate is calculated from the lowest- and highest-altitude data and an assumed air attenuation coefficient. The background count rate is due to contributions from the cosmic rays, airborne radon and its daughters, and equipment. The background is assumed to be independent of altitude, even though the cosmic-ray contribution increases slightly over these altitudes. Then, using this background value and the four lower-altitude data, a linear least-squares fit to $log \ (C_i - B)$ versus H produces the air attenuation coefficient. The uncertainty in the highest

altitude is usually quite large and so does not contribute a very useful data point to determine this coefficient. If the air attenuation coefficient is much different from the initial (assumed) value, the procedure is iterated until the background count rate and air attenuation coefficient change little from one iteration to the next and are consistent with the measured data.

Using this technique, a value exists for the background count rate that consists of contributions from airborne radon, cosmic rays, and equipment. The cosmic-ray and equipment contributions to the background count rate are assumed not to change during the survey, but the amount of radon (and its decay daughters) in the atmosphere will change daily. Therefore, the detectors are flown over the test line at the survey altitude at the beginning and end of each survey flight. Increases or decreases in the count rate compared to the altitude profile count rate represent increases or decreases in the background.

Before each flight, the voltage outputs from the NaI(Tl) detectors are matched in amplitude. This ensures that the same energy gamma ray in one detector produces an electrical pulse of the same size as a similar gamma ray makes in one of the other detectors. In other words, the width of the peak formed by gamma rays of the same energy will be a minimum, which is necessary to produce reliable results in the analysis stage.

During the data flights, the helicopter flew at 61 m (200 ft) AGL. At this altitude, the absorption by the air between the ground and the detectors was relatively small for the gamma rays of interest. The helicopter flew along predetermined lines spaced 91 m (300 ft) apart. This line spacing permits complete coverage of the survey area.

Immediately after each flight, a number of checks are performed to verify the reliability of the accumulated data. These checks are completed before the next flight begins. The detectors, electronics, and environmental instruments are checked to make sure that they are functioning properly. The data are also examined for surprises (such as areas of unexpected high-intensity radiation) that might change the data-acquisition strategy.

The test line data from the beginning and end of each flight provide an initial adjustment to the daily changes in nonterrestrial radiation. To check for more subtle variations, a portion of at least one line from each flight is reflown, and the data are compared to the data from the previous flights. This process serves as an additional check on data continuity and reproducibility.

20

APPENDIX C

DATA-ANALYSIS PROCEDURES

The body of this report provided an overview of the processes used to analyze the data for this survey. This appendix presents details of these processes for readers interested in a more precise description.

There are several methods for processing the data that may be used to evaluate the data. The most obvious is the GC method that is a simple integration of all gamma rays detected at each location. The GC method calculates the exposure rate for each sample and presents the results as a series of equal exposure contours on a map or photograph of the survey area. With this display, variations in the whole radiation field may be easily seen.

However, variations in the total radiation field are not always of most interest. Often what is important are the changes in isotopic concentrations (variations in the energy composition of the field) or the ability to track a single radioactive isotope throughout the survey area. The MMGC method is another integral-based analysis method. It is used to locate regions where the energy content of the gamma-ray spectrum deviates significantly from that of the natural background spectrum.

A third data-processing method often applied to the data is used to look for a specific isotope throughout the survey area. This method relies on mapping the observed count rate in a narrow energy window minus a suitably chosen background window to show how · that isotope is distributed throughout the survey area.

C.1 GROSS COUNT RATE

For the purpose of this survey, the GC of a gamma-ray energy spectrum is the integrated count rate in the energy range from 38–3,026 keV. The lower-energy limit is an effective lowest energy that can be reliably recorded by the airborne detector systems. There are almost no gamma rays of interest in these surveys having energies above the upper-energy limit. The exposure rate may be expressed as follows:

$$E_G = (C_G - B)\frac{e^{A(H-61)}}{930} \qquad \text{(C-1)}$$

where

A = the air attenuation coefficient (0.005387 m^{-1})

B = the background count rate at the survey altitude (counts/s)

C_G = the gross count rate at the survey altitude (counts/s)

E_G = the gamma-ray exposure rate (µR/h)

H = the aircraft height above the ground during the measurement (m)

The factor in parentheses $(C_G - B)$ is the net count rate (from terrestrial sources) for each 1-second data sample where C_G changes each second, and B is determined from the test-line data as discussed at the end of Appendix B. B is a measure (at the beginning and end of each flight) of the cosmic-ray, radon, and equipment and aircraft contributions to the radiation field at the flight altitude. The exponential factor corrects this net count rate for variations in altitude. (For example, if the aircraft is momentarily too high, this factor raises the net count rate to what it would have been if the aircraft had been at the desired survey altitude of 61 m [200 ft]).

The factor of 930 in the denominator is the conversion from counts per second measured at an altitude of 61 m (200 ft) to microroentgens per hour measured at 1 meter above the ground. This conversion factor depends on the measurements made at a 61-m (200 ft) altitude at the Lake Mohave Test Line in Nevada[11,12] and the air attenuation coefficient measured at the survey site. The conversion factor assumes a uniformly distributed radiation source over an area which is large compared to the detector's field of view and has an energy distribution similar to that of the natural background.

C.2 MAN-MADE GROSS COUNT RATE

The GC method maps the variations in the total radiation field. This is not always the most useful presentation of the data. Changes in the GC data may indicate the presence of man-made radionuclides or they may simply indicate changes in the radionuclide abundances caused by changes in the types of rocks. Similar changes in the GC data may be caused by an abrupt change in the vegetation coverage. For natural

background radiation, the shape (energy distribution) of the gamma-ray energy spectrum is generally fairly constant, and variations in the GC data can be represented by scaling the energy spectrum measured at one location to fit the new location.

The MMGC method is a means of identifying regions in the survey area where the shape of the energy spectrum deviates significantly from the shape of the background spectrum. Through its definition (presented below), the MMGC is very sensitive to small changes in the abundance of man-made isotopes while being very insensitive to large changes in the abundance of natural isotopes.

The technique relies on two basic characteristics. First, the energies of naturally occurring isotopes appear throughout the energy range where the system is designed to observe (40–4,000 keV). Second, man-made isotopes that have half-lives long enough for the isotope to be dispersed from their site of creation and then detected by an aerial survey generally have gamma-ray energies limited to less than about 1,400 keV. This energy is approximately midway between the 1,330-keV peak of ^{60}Co (a commonly observed man-made isotope) and the 1,460-keV peak of ^{40}K (a common naturally occurring isotope).

This situation can be exploited by measuring the gamma-ray spectrum in a background region—known to contain only naturally occurring isotopes. This background region provides a ratio of the low-energy to high-energy count rate that will be applied to succeeding measurements to find the count rate attributable to activity by man-made isotopes in the area. This process is good for locating regions of man-made isotopes, but it is also good for finding "false-positives"—regions that deviate from the originally measured background spectrum simply because they have different relative abundances of radioactive isotopes embedded in their rock formations. Usually, the number of regions identified by the MMGC method is small enough that the gamma-ray spectrum for each region can be inspected, and it can easily be determined which isotopes are present.

Using an energy spectrum from an area known to contain only naturally occurring radioactive isotopes, the ratio of the number of counts in the spectrum below a cutoff energy to those above that energy is defined as K_{MM}. Equation C-2 shows this ratio where the cutoff energy is generally 1,394 keV. Almost no gamma rays are observed beyond the ^{208}Tl peak at 2,614 keV, so an arbitrary upper limit of 3,000 keV (shifted up to 3,026 keV to match the upper edge of a particular

spectral channel) is generally chosen as the end of the high-energy range.

$$K_{MM} = \frac{\displaystyle\sum_{E=38}^{1394} c(E)}{\displaystyle\sum_{E=1394}^{3026} c(E)} \qquad \text{(C-2)}$$

where:

$c(E)$ = the counts in the background energy spectrum at the energy E

K_{MM} = the ratio of the low-energy counts to high-energy counts in the background spectrum

This ratio, assumed to be fairly constant over the survey area, is usually used throughout the survey area. (If there are drastic changes in the geology within the survey area, a different background spectrum may be needed for each of the geologically distinct regions.) The MMGC represents the integrated counts observed below the cutoff energy minus the integrated counts expected below the cutoff energy. The MMGC rate (C_{MM}) is given in Equation C-3:

$$C_{MM} = \sum_{E=38}^{1394} c(E) - K_{MM} \sum_{E=1394}^{3026} c(E) \qquad \text{(C-3)}$$

The other terms in the equation are defined above. In regions where there are no man-made isotopes, this equation reduces to statistical fluctuations about zero. In past studies, the MMGC method has been shown to be sensitive to low levels of man-made radiation (less than 1 μR/h) even in the presence of large variations in the natural background. In practice, this algorithm is a general search tool to locate regions of anomalous radioactivity.

C.3 GAMMA SPECTRAL ANALYSIS

The MMGC algorithm is very general and is sensitive to any change in the low-energy portion of the spectrum. It cannot tell us what causes the change—whether a true man-made isotope is present in this region; whether the increased low-energy gamma rays are caused by naturally occurring isotopes whose gamma rays underwent more inelastic scatterings before reaching the detectors (thus distorting the energy profile of the spectrum); or whether the isotopic composition of the background spectrum in this region of the survey is significantly different

22

from where K_{MM} was determined (for example, granite versus limestone). Once a region appears in the man-made contours, the energy spectrum is examined for individual isotopes. An analysis of the gamma spectrum will determine which isotopes are present and which of the three scenarios previously described caused the MMGC deviation.

Generally, the large background field (due to the naturally occurring isotopes) is not of interest—only the spectrum due to the man-made isotopes. Unfortunately for a 1-second spectrum, the number of counts at any given energy is so small as to make the identification of a particular isotope very difficult. To increase the number of counts in the spectrum (and thus produce better statistics), the spectra from neighboring locations are combined to produce a single spectrum showing the radiation measured over some larger area.

Figure C-1 shows how the "net" spectra shown throughout this report are defined. The area is divided into "peak" and "background" regions. The contour levels used to define the peak and background regions are usually MMGC levels since these are the man-made activity regions that are usually under investigation when creating these spectra. (The peak and background boundaries may be defined by several methods—contour levels or simple rectangular boxes may also be used.) The peak region of the spectrum consists of the spectra contained in the area bounded by the outer contour level. The background region consists of the spectra contained in the rectangular box but outside the outer contour level. This partitioning ensures that the background spectrum is representative of the geology near the anomaly, but there will be <u>some</u> contribution of man-made radioactivity in the background region. The net spectrum is the result of subtracting the background spectrum, normalized by the ratio of the peak live time to the background live time, from the peak spectrum.

$$c_{Net}(E) = c_{Peak}(E) - \frac{T_{Peak}}{T_{Bkg}} \ c_{Bkg}(E) \qquad (C\text{-}4)$$

where

$c_{Peak}(E)$ = the counts in the peak energy spectrum at the energy E

$c_{Bkg}(E)$ = the counts in the background energy spectrum at the energy E

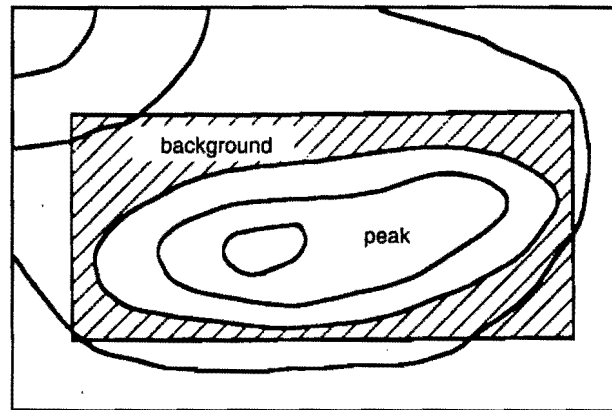$c_{Net}(E)$ = the counts in the net energy spectrum at the energy E

FIGURE C-1. *DEFINING PEAK AND BACKGROUND REGIONS AROUND RADIATION ANOMALIES. For the area shown, the peak region consists of all survey spectra within the rectangle and enclosed by the outer contour line. The background region consists of all spectra outside the outer contour line but inside the rectangle.*

T_{Peak} = the total live time for the spectrum comprised of all peak-region spectra (s)

T_{Bkg} = the total live time for the spectrum comprised of all background-region spectra (s)

This technique produces a net spectrum that has very little contribution from the naturally occurring radionuclides in the region and makes the identification of the remaining isotopes fairly easy. The one major drawback of the technique is that it does not necessarily produce a true indication of the strength of the isotopes seen in the net spectrum. That is, comparing the intensity of an isotope in one net spectrum with the intensity of the same isotope in another spectrum may not be very meaningful.

C.4 WINDOW ALGORITHMS

The algorithm employed in the search for a particular isotope is quite similar to the MMGC algorithm. The major difference is that only two or three small pieces of the spectrum are used instead of using the full gamma-ray energy spectrum. The two-window algorithm is the simplest of several window algorithms in use. It employs a narrow, primary window centered on the energy of the specific isotope's photopeak. A second window, located at higher energies, assumes that the background counts in the primary window are proportional to the counts recorded in the second window. The background window may abut the primary

window, or it may be separated from it in energy. The proportionality factor is determined in a region of the survey that does not contain any of the specific isotope so that the number of counts in the primary window is directly related to the number of counts in the background window. The following equation is for the two-window algorithm:

$$C_{2-Window} = \sum_{E=E_1}^{E_2} c(E) - K_2 \sum_{E=E_3}^{E_4} c(E) \qquad \text{(C-5)}$$

where

$C_{2-Window}$ = the net counts in the primary window

$c(E)$ = the counts in the gamma-ray energy spectrum at the energy E

E_n = the limiting energies of the windows $(E_1 < E_2 \le E_3 < E_4)$

K_2 = the ratio of the counts in the primary window to the counts in the background window in a clean region of the survey area

If the principle source of background gamma rays in the primary window is from scattered gamma rays from photopeaks at higher energies, then this is a reasonable assumption. If there are isotopes other than the one of interest with photopeaks in the primary window, then this algorithm will fail. For example, ^{234m}Pa is a member of the ^{238}U decay chain, and ^{228}Ac is a member of the ^{232}Th decay chain. Both of these radionuclides occur naturally and both have several gamma rays in the 910- to 970-keV range. Attempting to map the distribution of one radionuclide using a window in this energy range produces very marginal results since it is very difficult to determine whether changes in the count rate are caused by fluctuations in the isotope of interest or by fluctuations in the concentration of the other isotope.

If a region that is free of the specific isotope cannot be found or if the composition of the other isotopes changes drastically in the clean region, then a simple multiplicative factor will not relate the counts in the primary window to the counts in the background window. To ease this problem, the three-window algorithm employs a background window on each side of the primary window. (The two background windows generally abut the primary window in energy.) This algorithm assumes that, for any spectrum, the number of

background counts in the primary window is linearly related to the counts in the two background windows. The following equation is for the three-window algorithm:

$$C_{3-Window} = \sum_{E=E_2}^{E_3} c(E) - K_3$$

$$\left[\sum_{E=E_1}^{E_2} c(E) + \sum_{E=E_3}^{E_4} c(E) \right] \qquad \text{(C-6)}$$

where

$C_{3-Window}$ = the net counts in the primary window

$c(E)$ = the counts in the gamma-ray energy spectrum at the energy E

E_n = the limiting energies of the windows $(E_1 < E_2 < E_3 < E_4)$

K_3 = the ratio of the counts in the primary window to the counts in the two background windows in a clean region of the survey area

The three-window algorithm is also very useful in extracting low-energy photopeak counts where the shape of the Compton-scatter contributions from other isotopes is changing significantly. The three-window algorithm is commonly used to extract the counts in the ^{137}Cs photopeak.

C.5 SENSITIVITY

The correlation of photopeak gammas (uncollided in soil or air but totally absorbed in the detector) to soil activity may be treated analytically in a simple manner whereas the total or gross count may not. The general equations used to compute the photopeak count rates per unit soil activity and per unit point source are described in the following section.

C.5.1 Area Source

Assuming a vertical activity distribution in the soil,

$$S(z) = S_{E0} \, e^{-az} \qquad \text{(C-7)}$$

where

S_{E0} = the activity concentration at the surface of the soil (γ/cm^{3}s)

α = exponential concentration factor (1/cm)

z = depth in the soil (cm)

The sensitivity, X_E [cps/(γ/cm^{3}s)], to a monoenergetic gamma distribution may be written as follows (see reference 13 for a derivation):

$$X_E = \frac{A_0}{2} \int_{\theta=0}^{90^0} \frac{R(\theta)\ \tan\theta\ e^{-\left(\frac{\mu}{\rho}\right)_a \rho_a h \sec\theta}}{\alpha + \left(\frac{\mu}{\rho}\right)_s \rho_s\ \sec\theta}\ d\theta \qquad \text{(C-8)}$$

where

A_0 = detector effective area for monoenergetic gamma total absorption in the detector for fluence perpendicular to the ground (cm^2)

$R(\theta)$ = relative effective area versus angle, θ, measured from the perpendicular to the ground

$\left(\frac{\mu}{\rho}\right)_a$ = air mass attenuation coefficient (cm^2/g)

$\left(\frac{\mu}{\rho}\right)_s$ = soil mass attenuation coefficient for the specific gamma energy (cm^2/g)

h = detector altitude above the ground (cm)

ρ_a = air density (g/cm^3)

ρ_s = soil density (g/cm^3)

In practice, the effective area, A_0, and angular factor, $R(\theta)$, are measured in the laboratory.

The following are other useful conversions:

A. The activity concentration per unit soil surface area:

$$S_A = \frac{S_{E0}}{\alpha} \qquad \text{(C-9)}$$

B. The activity concentration per unit soil surface mass:

$$S_\rho^0 = \frac{S_{E0}}{\rho} \qquad \text{(C-10)}$$

C. The activity concentration to a soil sample of depth z:

$$S_\rho^z = S_{E0}\ \frac{1 - e^{-\alpha z}}{\rho \alpha z} \qquad \text{(C-11)}$$

C.5.2 Point Sources

Point-source sensitivity is a simple computation if one assumes that the detector passes over the source to achieve a minimum source–detector distance and that the gamma fluence rate changes little during a 1-second data-acquisition time at the minimum source–detector distance. These conditions generally exist during a routine survey:

$$X_\rho = A_0 \frac{e^{-\left(\frac{\mu}{\rho}\right)_a \rho_a h}}{4\pi h^2} \qquad \text{(C-12)}$$

Parameters have previously been established, and the sensitivity units are counts in the photopeak per emitted gamma.

Since point-source gammas are detectable at angies of other than zero degrees (or directly above the source) and when a source is weak (less than a millicurie), a sum of several data points may be required. The value of X_ρ then decreases, but the MDA increases.

REFERENCES

1. Apt, K.E. and V.J. Lee. *Environmental Surveillance at Los Alamos During 1975*. LANL Report No. LA-6321-MS, Los Alamos, New Mexico; 1976.

2. Ahlquist, A.J.; A.K. Stoker; and L.K. Troki. *Radiological Survey and Decontamination of the Former Main Technical Area (TA-1) at Los Alamos, New Mexico*. LANL Report No. LA-6887, Los Alamos, New Mexico; 1977.

3. Mayfield, D.L.; A.K. Stoker; and A.J. Ahlquist. *Radiological Survey of the Bayo Canyon, Los Alamos, New Mexico*. DOE Report No. DOE/EV-0005/15, Los Alamos, New Mexico; 1979.

4. Environmental Surveillance Group. *Environmental Surveillance at Los Alamos During 1981*. Los Alamos Report No. LA-9349-ENV, Los Alamos, New Mexico; 1982.

5. Fritzsche, A.E. *An Aerial Radiological Survey of Technical Area 15 and Surroundings, Los Alamos National Laboratory*. Report No. EGG-10282-1095, EG&G/EM, Las Vegas, Nevada; 1989.

6. Fritzsche, A.E. *An Aerial Radiological Survey of Technical Areas 2, 21, and 53 and Surroundings, Los Alamos National Laboratory*. Report No. EGG-10617-1030, EG&G/EM, Las Vegas, Nevada; 1990.

7. Los Alamos Aerial Survey; EG&G/EM, Las Vegas, Nevada; 1975 [unpublished].

8. Guillou, R.B. *Albuquerque –Los Alamos Area (ARMS-II)*. Report No. CEX-61.6.2, EG&G, Inc., Santa Barbara, California; 1964.

9. Lindeken, C.L.; K.R. Peterson; D.E. Jones; and R.E. McMillen. "Geographical Variations in Environmental Radiation Background in the United States," *Proceedings of the Second International Symposium on the Natural Radiation Environment, August 7–11, 1972, Houston, Texas*. National Technical Information Service, Springfield, Virginia; 1972, pp 317–332.

10. Klement, Jr., A.W.; C.R. Miller; R.P. Minx; and B. Shleien. *Estimates of Ionizing Radiation Doses in the United States 1960-2000*. U.S. EPA Report ORP/CSD72-1, EPA, Washington, D.C.; 1972.

11. Mohr, R. [Interoffice memorandum, subject: Ion Chamber Measurements at the Bonelli Bay Calibration Range, EG&G/EM, Santa Barbara, California]. February 11, 1980.

12. Mohr, R. [Interoffice memorandum, subject: Ground Measurements at the Bonelli Bay Calibration Range, EG&G/EM, Santa Barbara, California]. April 6, 1981.

13. Reiman, R.T. *In Situ Surveys of the U.S. Department of Energy's Rock Flats Plant, Golden, Colorado*. Report No. EGG–10617–1129. EG&G/EM, Las Vegas, Nevada, 1991.

DISTRIBUTION

DOE/DP

J. A. Weidner, LCDR USN (1)

DOE/NSIC

R. S. Scott (1)

DOE/NV

K. D. Lachman (1)

LANL

E. Van Eeckhout (3)

BN

H.W. Clark, Jr.	LVAO	(1)
P. P. Guss	WAMO	(1)
R. K. Kulm	LVAO	(1)
K. R. Lamison	LVAO	(1)
J. T. Mitchell	LVAO	(1)
A. J. Will	LVAO	(1)

RESOURCE CENTERS

Public Reading Room	(1)
RSL	(30)
TIRC	(1)
WAMO	(1)

OSTI (2)

AN AERIAL RADIOLOGICAL SURVEY OF THE
LOS ALAMOS NATIONAL LABORATORY
AND SURROUNDING AREA
LOS ALAMOS, NEW MEXICO
DOE/NV/11718-107
DATE OF SURVEY: MAY 1994
DATE OF REPORT: MARCH 1998